INTERNATIONAL JOURNAL FOR NUMERICAL METHODS IN FLUIDS, VOL. 12, 747–763 (1991)

NUMERICAL COMPUTATION OF FLUID PRESSURE TRANSIENTS IN PUMPING INSTALLATIONS WITH AIR ENTRAINMENT

T. S. LEE

Mechanical Engineering Department, Faculty of Engineering, National University of Singapore, Singapore 0511

SUMMARY

In pumping installations such as sewage pumping stations, where gas content and air entrainment exist, the computation of fluid pressure transients in the pipelines becomes grossly inaccurate when constant wave speed and constant friction are assumed. A numerical model and computational procedure have been developed here to better compute the fluid pressure transient in a pipeline by including the effects of air entrainment and gas evolution characteristics of the transported fluid. Free and dissolved gases in the fluid and cavitation at the fluid vapour pressure are modelled. Numerical experiments show that entrained, entrapped or released gases amplify the pressure peak, increase surge damping and produce asymmetric pressure surges. The transient pressure shows a longer period for down-surge and a shorter period for up-surge. The up-surge is considerably amplified and the down-surge marginally reduced when compared with the gas-free case. These observations are consistent with the experimental observations of other investigators. Numerical experiments also show that the use of a variable loss factor in the pressure transient analysis produces marginally higher maximum and lower minimum pressure transients when compared with the constant-loss-factor model for pipelines where the pressures are above the fluid vapour pressure.

KEY WORDS Pressure transient Variable wave speed Air entrainment

INTRODUCTION

Pumping stations commonly work according to the on–off principle whereby the automatic starting and stopping of pumps are governed by the pump well level and load demand. Flow changes through the pumps give rise to transient pressures in the pipelines, which have to be considered in order to prevent failure of the pipelines. The case of stoppage of one or more pumps simultaneously due to power failures or operational conditions with check valves in the pumping station might cause substantial high and low pressures. At the design stage these pressures have to be analysed and suitable surge suppression devices proposed, or an alternative route has to be chosen so as to minimize the pressure surge to within suitable levels. The analysis is usually based on the assumptions of no air in the water and a constant friction factor of the pipeline. However, in some pumping installations, such as sewage pumping stations, air entrainment into the system can occur as a result of: falling jets of sewage from the comminutors into the sump near the operating pump bellmouths; attached vortex formation arising from the operation of the pumps; and the adverse flow path towards the operating pumps. Air may also be admitted into the pipeline by vortex action in an inadequately designed air vessel. Trapped air pockets at the top of the pipe cross-section at high points along the pipe profile can also be present owing to the

0271–2091/91/080747–17$08.50 *Received February 1990*

incomplete removal of air during the commissioning and filling-up operation or the progressive upward migration of pockets of air. The flow in the pipelines would also contain free gas, although the volumetric proportion may be small, and most liquid also contains dissolved gases in solution. Gas bubbles will be evolved from the liquid during the passage of low-pressure transients. When the liquid is subject to high transient pressures, the free gas will be compressed and some may be dissolved. The process is highly time- and pressure-dependent. The resulting pressure transients with air entrainment and gas release are considerably different from those computed according to models with no air and constant friction factor.

In general, the transient flow in a pipeline can be divided into three phases: waterhammer, cavitation and column separation. In the waterhammer phase the release of dissolved gas is small and the wave speed depends on the void fraction, which in turn depends on the local pressure. In the cavitation phase, gas bubbles are dispersed throughout the liquid owing to the reduction of the local transient pressures to the vapour pressure of the liquid. The liquid boils at that pressure and the local pressure will not fall further. The liquid in this phase behaves like a gas–liquid mixture. Depending upon the pipeline geometry and velocity gradient, the gas bubbles may become so large as to fill the entire cross-section of the pipe. This is the column separation phase. The existence of column separation, trapped gas volumes and entrained free gas bubbles greatly complicates the transient analysis by making the transient wave speed a function of the transient pressure. In practice, the analysis is also made more difficult owing to lack of information such as: the location and size of trapped air pockets in the pipelines; the amount of free air bubbles distributed throughout the liquid; and the rate of gas release and absorption in the liquid as a function of pressure and time. This two-phase flow problem has been the subject of much research in recent years.

Whiteman and Pearsall[1,2] were the first to study the effects on pressure transients when air is entrained into the fluid of a pumping station. Pump shut-down tests were conducted with reflux valve closure on two sewage pumping stations with air entrained into the fluid. In general, the first pressure peak with entrained air in the pipeline was found to be higher than that predicted by the constant-wave-speed waterhammer theory. Two different types of air entrainment models have been proposed in the literature for predicting the above-transient pressure behaviour: the concentrated vaporous cavity model[3,4] and the air release model.[5–7] The concentrated vaporous cavity model confines the vapor cavities to fixed computing sections and uses a constant wave speed for the fluid in reaches between the cavities. The air release model assumes the evolved and free gas to be distributed homogeneously throughout the reaches, thereby requiring variable wave speeds which are dependent on gas content and local pressure. The concentrated vaporous cavity model produces satisfactory results in slow transients but unstable solutions for rapid transients, e.g. pump stoppage with reflux valve closure with air content. The air release model produces satisfactory results in pump shut-down cases but is susceptible to numerical damping.[8,9] This damping introduced in the numerical method may give a distorted magnitude of the transient pressure damping characteristics due to losses, friction or wave speed variations.

AIR ENTRAINMENT AND GAS RELEASE VARIABLE-WAVE-SPEED MODEL

Various earlier investigators[3,10–21] have observed that the presence of undissolved gas bubbles in a fluid greatly reduces the wave speed. The effect of free air on the wave speed is more significant at low-pressure conditions, where its volume is greater than at high-pressure conditions. The variable-wave-speed model proposed here assumes the presence of a free entrained air content ε_0 and a dissolved gas content ε_g in the liquid at atmospheric pressure. Assumptions are made that: the gas–liquid mixture is homogeneous; the free gas bubbles in the liquid follow a polytropic

compression law with $n = 1{\cdot}2$–$1{\cdot}3$; and the pressure within the air bubbles during the transient process is in equilibrium with the local fluid pressure. When the computed local transient pressure falls below the fluid gas release pressure p_g, an instantaneous release of a dissolved gas content ε_g is assumed. The local pressure remains constant and is equal to the vapour pressure. When the computed transient pressure recovers to a value above the gas release pressure, an equivalent amount of released gas content is assumed to have redissolved into the liquid. Since the local pressure remains constant when the computed pressure is below the gas release pressure, the maximum air content has a limit and hence the wave speed has a lower limit in the model proposed which is determined by this air content at the vapour pressure condition.

Consider a mass of liquid containing a fractional volume of gas in free bubble form, ε, the volume of the gas plus liquid being V_t. The volume of liquid is

$$V_l = (1-\varepsilon)V_t \tag{1}$$

and the free gas volume is

$$V_g = \varepsilon V_t. \tag{2}$$

On applying a pressure increment Δp to the liquid, the liquid volume will change to

$$V_l^* = (1-\Delta p/K)(1-\varepsilon)V_t. \tag{3}$$

The gas volume is assumed to be distributed in small-bubble form and to have a polytropic change in properties due to partial heat being transferred to the water. Any gas volume change will therefore be related through

$$p(V_g)^n = (p+\Delta p)(V_g^*)^n, \tag{4}$$

where V_g^* is the fractional gas volume at pressure $p+\Delta p$. The volume of the gas–liquid mixture at pressure $p+\Delta p$ will therefore become

$$V_t^* = \left(\frac{p}{p+\Delta p}\right)^{1/n} \varepsilon V_t + \left(1-\frac{\Delta p}{K}\right)(1-\varepsilon)V_t. \tag{5}$$

With the smaller terms neglected,

$$\frac{V_t^*}{V_t} = 1 - \left(\frac{\varepsilon}{n}\frac{\Delta p}{p} + \frac{\Delta p}{K}\right). \tag{6}$$

Hence the effective bulk modulus of the fluid with an air fraction content ε at a pressure p is given by

$$K^* = \frac{\Delta p}{1 - V_t^*/V_t} = \frac{1}{1/K + \varepsilon/np}. \tag{7}$$

The effective bulk modulus of the gas–liquid mixture, K_T, including the pipe distensibility effect and pipe constraint condition c, is thus given by

$$\frac{1}{K_T} = \frac{1}{K} + \frac{\varepsilon}{np} + \frac{cD}{eE}. \tag{8}$$

Hence at the ith node point and kth time level, as shown in Figure 1, the local wave speed a_i at an absolute pressure p_i with an air fraction content ε_i is given by

$$a_i^k = \left[\rho_w(1-\varepsilon_i^k)\left(\frac{1}{K} + \frac{\varepsilon_i^k}{np_i^k} + \frac{cd}{eE}\right)\right]^{-1/2}. \tag{9}$$

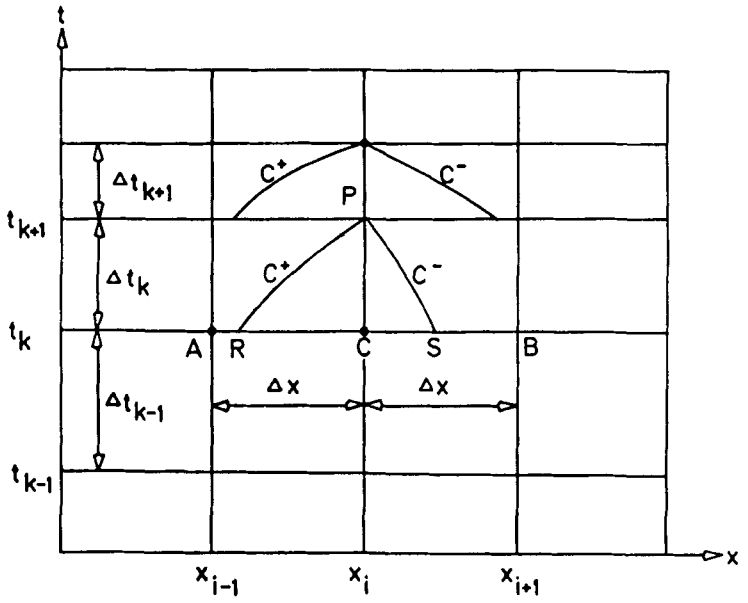

Figure 1. Computational grid

For this model of variable wave speed the initial free air fraction ε_0 and the dissolved gas fraction ε_g at a reference absolute pressure p_0 must be specified. The initial variable wave speed along a pipeline ($i=0, 1, \ldots, N$) is then computed through the absolute pressure distribution along the pipeline from equation (9) at $k=0$ (steady state).

The transient computation of the fraction of air content along the pipeline depends on the local pressure and local air volume and is given by

$$\varepsilon_T^{k+1} = \left(\frac{p_i^k}{p_i^{k+1}}\right)^{1/n} \varepsilon_i^k \quad \text{and} \quad \varepsilon_0^{k+1} = \left(\frac{p_0}{p_i^{k+1}}\right)^{1/n} \varepsilon_0 \tag{10a}$$

for $p_i^{k+1} \geqslant p_g$ and $\varepsilon_T^{k+1} \leqslant \varepsilon_0^{k+1} + \varepsilon_g$,

$$\varepsilon_i^{k+1} = \varepsilon_T^{k+1} \tag{10b}$$

for $p_i^{k+1} \geqslant p_g$ and $\varepsilon_T^{k+1} > \varepsilon_0^{k+1} + \varepsilon_g$,

$$\varepsilon_i^{k+1} = \left(\frac{p_i^k}{p_i^{k+1}}\right)^{1/n} (\varepsilon_i^k - \varepsilon_g) \tag{10c}$$

for $p_i^{k+1} < p_g$,

$$\varepsilon_i^{k+1} = \left(\frac{p_i^k}{p_g}\right)^{1/n} (\varepsilon_i^k + \varepsilon_g). \tag{10d}$$

This air fraction content is then inserted in equation (9) to compute the wave speed along the pipeline for the next time level computation. In this variable-wave-speed model no limit is set for the lowest wave speed value. The model computes the lowest values based on the minimum system pressure allowable for a real system. For water saturated at atmospheric pressure the gas release pressure head approaches that of the vapour pressure (i.e. 2.4 m water absolute). The

typical free air content in sewage at atmospheric pressure is about 0·1% and the free gas content evolved at the gas release head is about 2·0% at atmospheric head.[4, 17, 22, 23]

VARIABLE LOSS FACTOR f_l IN THE METHOD OF CHARACTERISTICS

There is experimental evidence[24–29] which demonstrates that losses due to friction, fittings, etc. are affected by unsteadiness in the flow. The unsteadiness in the flow affects the turbulence, boundary layer velocity profiles and hence the losses. Kita *et al.*[30] showed experimentally that in very slow transients the quasi-steady approximation of losses due to friction can be used with satisfactory accuracy. Recent research evidence has shown that for more rapid transients the unsteady flow friction factor is greater than the steady flow friction factor in accelerated flows, and the converse for decelerated flows.[30] For such flows an appropriate representation of the unsteady loss factor and frictional effects is necessary. A review of the available literature indicates that satisfactory theoretical loss models have been developed for unsteady laminar and single-phase flow,[31–34] while no satisfactory model is available for unsteady turbulent and two-phase flow.[35]

Thus a modified variable-loss-factor model is proposed here for the study of unsteady pressure transient flow with air entrainment and gas release problems. The present model takes into account the losses due to the two-phase nature of the flow and the features of the pipelines. This model was tested for the case of pump trips due to power failures and valve closure in sewage pumping stations. For the variable-loss-factor model proposed here the results show that the maximum pressure transient is marginally higher and the minimum pressure transient is marginally lower than for the corresponding model with a constant steady state loss factor.

The loss factor (f_l) model proposed for use in conjunction with the method of characteristics with air entrainment and gas release in a pipeline system can be evaluated at a local point i as follows:

(a)
$$Re_i = V_i D_i / \nu_i \quad \text{(local effective Reynolds number)},$$
$$\nu_i = (1-\varepsilon_i)\nu_s + \varepsilon_i \nu_g. \tag{11}$$

(b) Assume
$$(K_{\text{loss}})_i = K_m(Re_i) + K_f(Re_i),$$
$$K_m(Re_i) = \text{local loss factor due to pipe features},$$
$$K_f(Re_i) = (\Delta x_i / D_i) f(Re_i).$$

The total losses at a node point are thus represented by

$$\sum_i (K_{\text{loss}})_i \left(\frac{V_i |V_i|}{2g} \right). \tag{12}$$

(c)
$$Re_i \leqslant 1, \qquad f(Re_i) = 64,$$
$$1 \leqslant Re_i \leqslant 2000, \qquad f(Re_i) = 64/Re_i,$$
$$Re_i > 2000, \qquad (f_i)^0 = f \quad \text{(Moody's formula[36])}.$$

The value of $f(Re_i)$ is obtained through iteration of the corresponding Colebrook–White equation[7, 37] with the appropriate roughness factor for the pipe at the node point i.

(d) For $|[f(Re_i)-(f_i)^0]/f(Re_i)| \geqslant 0{\cdot}001$, set $(f_i)^0 = f(Re_i)$ and repeat iteration.
(e) Hence a local loss factor $(f_l)_i$ is then defined as

$$(f_l)_i = (K_{loss})_i\,(D_i/\Delta x_i). \tag{13}$$

The steady state overall loss factor at the operating point of a system can be determined from the pump characteristic curve and the system curve. This value is used as a check against the value obtained from equation (13) for the summation of $i=0, 1, \ldots, N$ at the steady state Reynolds number.

METHOD OF CHARACTERISTICS WITH a_i AND $(f_l)_i$

The method of characteristics applied to the pressure transient problem with variable wave speed and variable loss factor as modelled above can be described by the following C^+- and C^--characteristic equations:

C^+-characteristic equations,

$$\frac{g}{a}\frac{dH}{dt}+\frac{dV}{dt}+\frac{g}{a}V\sin\alpha+\frac{f_l}{2D}V|V|=0, \tag{14}$$

$$dx/dt = V+a; \tag{15}$$

C^--characteristic equations,

$$-\frac{g}{a}\frac{dH}{dt}+\frac{dV}{dt}+\frac{g}{a}V\sin\alpha+\frac{f_l}{2D}V|V|=0, \tag{16}$$

$$dx/dt = V-a. \tag{17}$$

With reference to the irregular time and regular x grid notation used in Figure 1, i denotes the regular x-mesh point value at location $x=(i\Delta x)$ and k denotes the irregular time level corresponding to time $t_k=\sum\Delta t_k$. The value of the time step Δt_k at each time level is determined by the CFL criterion

$$\Delta t_k = \min\,[k_i\Delta x/(|V_i|+a_i)] \quad \text{for } i=0, 1, \ldots, N, \tag{18}$$

where k_i is a constant less than unity.

The characteristic equations specified by (14)–(17) can thus be approximated by simple finite difference expressions. The approach used here is a variation of the well-known 'method of specified time interval'.[7,38–40] In the present execution the time interval Δt_k at each time level $t_k=\sum\Delta t_k$ is allowed to vary according to equation (18). With reference to Figure 1, the finite difference approximations for the characteristic equations are

$$\frac{g}{a_R}\frac{H_i^{k+1}-H_R}{\Delta t_k}+\frac{V_i^{k+1}-V_R}{\Delta t_k}+\frac{g}{a_R}V_R\sin\alpha_i+\frac{f_{l_R}}{2D}V_R|V_R|=0, \tag{19}$$

$$\frac{x_i-x_R}{\Delta t_k}=V_R+a_R, \tag{20}$$

$$-\frac{g}{a_S}\frac{H_i^{k+1}-H_S}{\Delta t_k}+\frac{V_i^{k+1}-V_S}{\Delta t_k}-\frac{g}{a_S}V_S\sin\alpha_i+\frac{f_{l_S}}{2D}V_S|V_S|=0, \tag{21}$$

$$\frac{x_i-x_S}{\Delta t_k}=V_S-a_S, \tag{22}$$

where R is the point of interception of the C^+-characteristic line on the x-axis between node points $i-1$ and i at the kth time level, and S is the interception of the C^--characteristic line on the x-axis between i and $i+1$. With conditions known at points $i-1$, i and $i+1$ at the kth time level, the conditions at R and S can be evaluated by a linear interpolation procedure. The conditions at R and S are then substituted into equations (19)–(22) and the solutions at the next, i.e. $(k+1)$th, time level at point i are obtained for $i=0, 1, \ldots, N$. A mesh size of $N=1000$ was used for the solutions presented in this work.

BOUNDARY CONDITIONS

A common flow arrangement in water and sewage engineering consists of a lower reservoir, a group of pumps with a check valve in each branch, and a pipeline discharging into an upper reservoir (water tower, gravity conduit, aeration well, etc.). In order to safeguard the pipeline and its hydraulic components from over- and/or underpressurization, it is important to determine extreme pressure loads under transient conditions. Pump stoppage is an operational case which has to be investigated and which often gives rise to maximum and minimum pressures. The most severe case occurs when all the pumps in a station fail simultaneously due to power failure. In this case the flow in the pipeline rapidly diminishes to zero and then reverses. The pump also rapidly loses its forward rotation and reverses shortly after the reversal of the flow. As the pump speed increases in the reverse direction, it causes great resistance to the back flow, which produces high pressure in the discharge line near the pump. To prevent reverse flow through the pump, a check valve is usually fitted immediately after each pump. When the flow reverses, the check valve is activated and closed. A large pressure transient occurs in the pipeline when the flow reverses, and the check valves of the pumps close rapidly.

The equivalent pump characteristics in the pumping station during pump stoppage and pump run-down can be described by the homologous relationship for n_p pumps as follows:

$$H_e^{k+1} = A_1(N^{k+1})^2 + (A_2/n_p)(N^{k+1})\,Q_0^{k+1} + (A_3/n_p^2)(Q_0^{k+1})^2, \tag{23}$$

$$T_e^{k+1} = B_1 n_p (N^{k+1})^2 + B_2(N^{k+1})Q_0^{k+1} + (B_3/n_p)(Q_0^{k+1})^2, \tag{24}$$

$$\eta_e^{k+1} = C_1 + (C_2/n_p)(Q_0^{k+1}/N^{k+1}) + (C_3/n_p^2)(Q_0^{k+1}/N^{k+1})^2, \tag{25}$$

$$T_e = -I_e\,\mathrm{d}\omega/\mathrm{d}t, \tag{26}$$

where $H_0^{k+1} = H_e^{k+1}$, $I_e = n_p I$, $\omega = 2\pi N$, Q is the flow rate; n_p is the number of pumps, A_1, A_2, A_3, B_1, B_2, B_3 and C_1, C_2, C_3 are single-pump constants and H_e, T_e and η_e are the equivalent pump head, torque and efficiency respectively. The efficiency of the equivalent pump during pump run-down is assumed equal to the efficiency of the corresponding single-pump run-down efficiency. Equation (23) is to be solved together with the C^--characteristic line described by equations (21) and (22) for a pump speed N^{k+1} determined from equations (24)–(26) by the procedures following Fox,[7] using the concept of an equivalent pump when there is more than one pump operating in a pumping station. The changes in pump speed during pump run-down for both normal and turbine modes are modelled. When reversed flow is encountered in the pump, the check valve is assumed closed. At this instant, V_0^{k+1} is assumed zero for the C^--characteristic line at $i=0$ for all subsequent time levels. In the case where the check valve closing time is known, the flywheel or pump set inertia can be sized such that the pump continues delivery for a period longer than the check valve closure time. This will ensure non-reversal of flow before the check valve is able to close. Downstream of each of the above profiles is assumed a constant-head reservoir, i.e. H_N^{k+1} = constant for all time levels, and this is solved with the C^+-characteristic line for V_N^{k+1} for each time level.

DISCUSSION

A typical pipeline profile of a sewage pumping station is shown in Figure 2. Figure 3 shows the effect of air entrainment and gas release in the variable-wave-speed model on the pressure transient when compared with that using a constant-wave-speed model with no air content. It shows that released gas and entrained air increase the maximum pressure up-surge along the pipeline and reduce the magnitude of the negative pressure down-surge. A study of the many corresponding numerical experiments using the variable-wave-speed model shows three distinct characteristic differences of pressure surge at an unprotected pumping station following power failure and instantaneous closure of the check valve when the flow reverses: (a) the first pressure peak is above that predicted by the constant-wave-speed model and the transient times differ, (b) the damping of the surge pressure is noticeably larger when compared with the constant-wave-speed model, (c) the surges are asymmetric with respect to the static head, while the pressure transients for the constant-wave-speed model are symmetric with respect to the static head. If there is evolution and subsequent absorption of gas in the liquid along the pipeline, the initial up-surge caused by valve closure at the pumping station may be small but is very often followed by a delayed substantial pressure up-surge. This delayed substantial pressure up-surge due to gas release at the gas release head along the pipeline was also observed by Clarke.[41] The arrival of this substantial pressure up-surge at the pumping station generates a positive transient which travels upstream towards the reservoir. This positive transient raises the pressure along the pipeline and causes the free gas present in the flow to dissolve, thus increasing the effective bulk modulus and the wave speed (Figure 4). This positive pressure wave is then reflected off the downstream reservoir as a negative pressure wave. Owing to the higher pressure upstream of the reservoir, this negative pressure wave travels rapidly and arrests the high-pressure up-surge at the

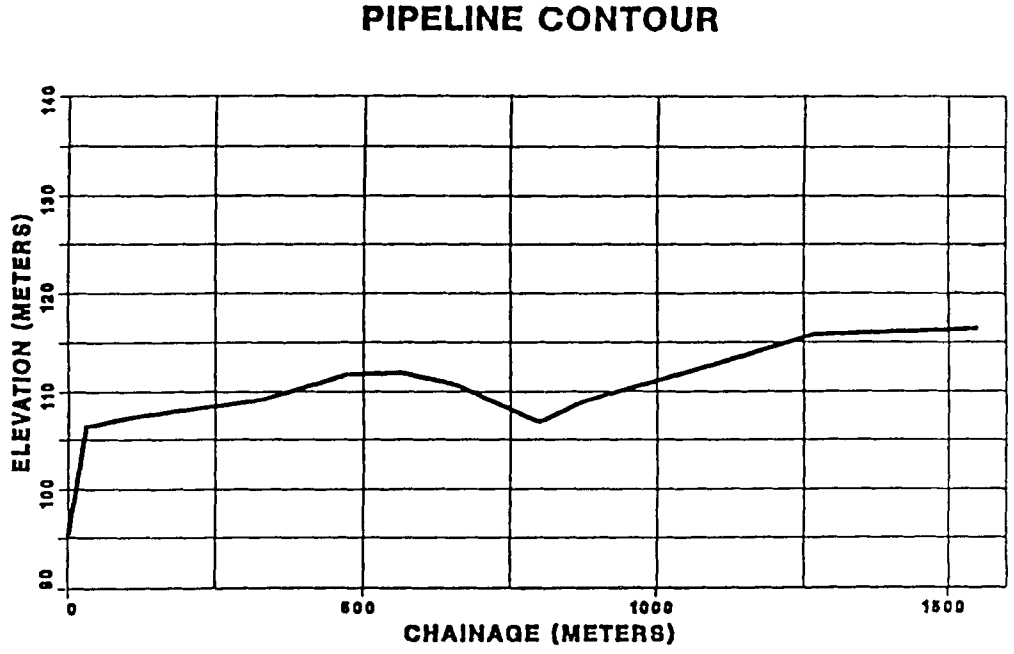

Figure 2. Pipeline contour of pumping station

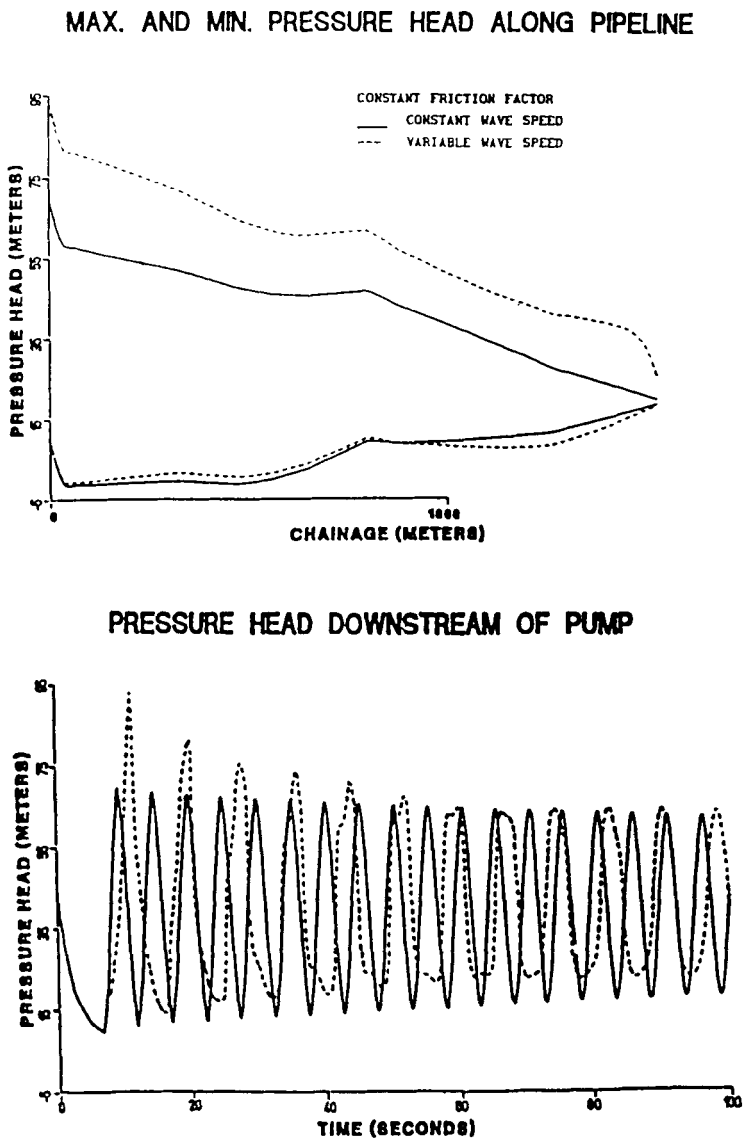

Figure 3.

pumping station. Hence the substantial pressure up-surge is present only for a short duration. As the surge damping due to losses and the presence of air sets in, the pressure down-surge along the pipeline usually does not subsequently fall below the gas release head, and a regular oscillating pressure surge will then be observed. Hence the entrainment of free air and the release of gas at the gas release head reduce the local wave speed considerably (Figures 3 and 4) and produce a complicated phenomenon of reflection of pressure waves off these 'cavities'. The lower local wave speed also increases the duration of the pressure down-surge as compared with the duration of the pressure up-surge.

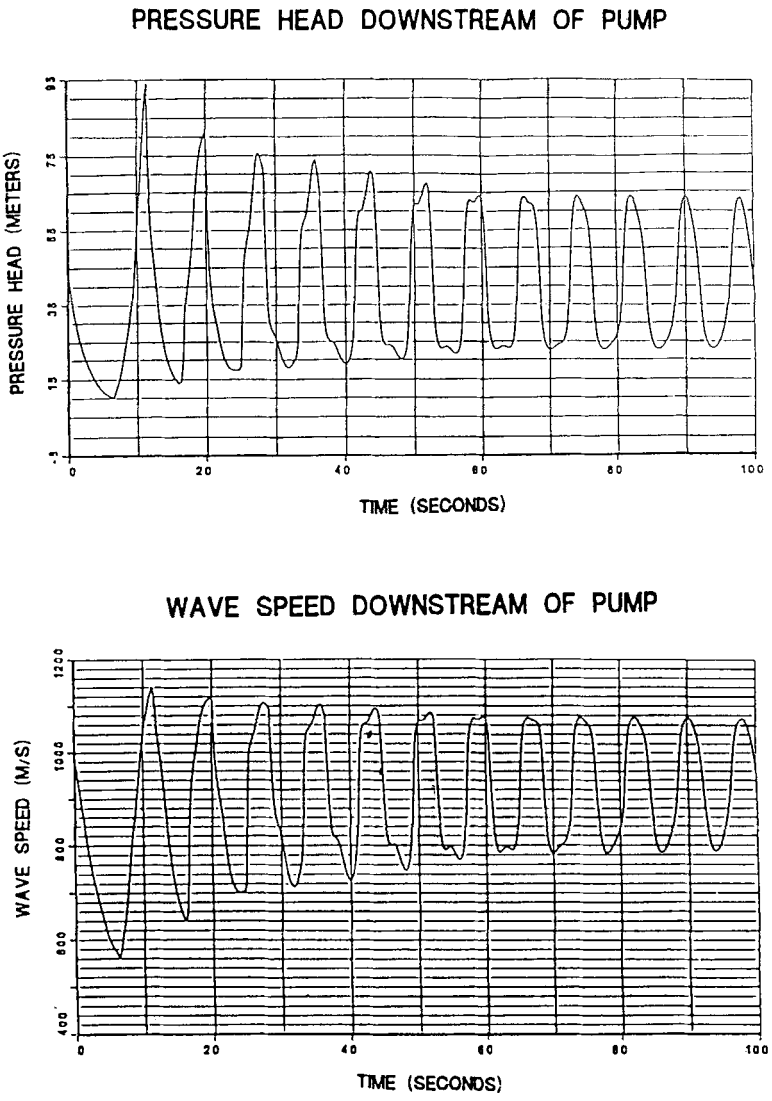

Figure 4.

The above characteristics were also observed experimentally by Whiteman and Pearsall,[1,2] Dawson and Fox[42] and Jonsson.[9] There are several reasons given in the literature for the increase in peak pressure during the pressure transient with air entrainment. Jonsson attributed the increase to the compression of 'an isolated air pocket' in the flow field after the valve closure. Dowson and Fox attributed it to the 'cumulative effect of minor flow changes during the transient'. From the numerous numerical experiments performed on the variable-wave-speed model, we observed that the greater peak pressure obtained for the variable-wave-speed model is due to the fact that a lower average wave speed delays the wave reflection at the reservoir and thus allows a more complex variation in pressure interaction to occur in the system, culminating in a peak at a specific transient interval. Falconer *et al.*[43] showed similarly through computer

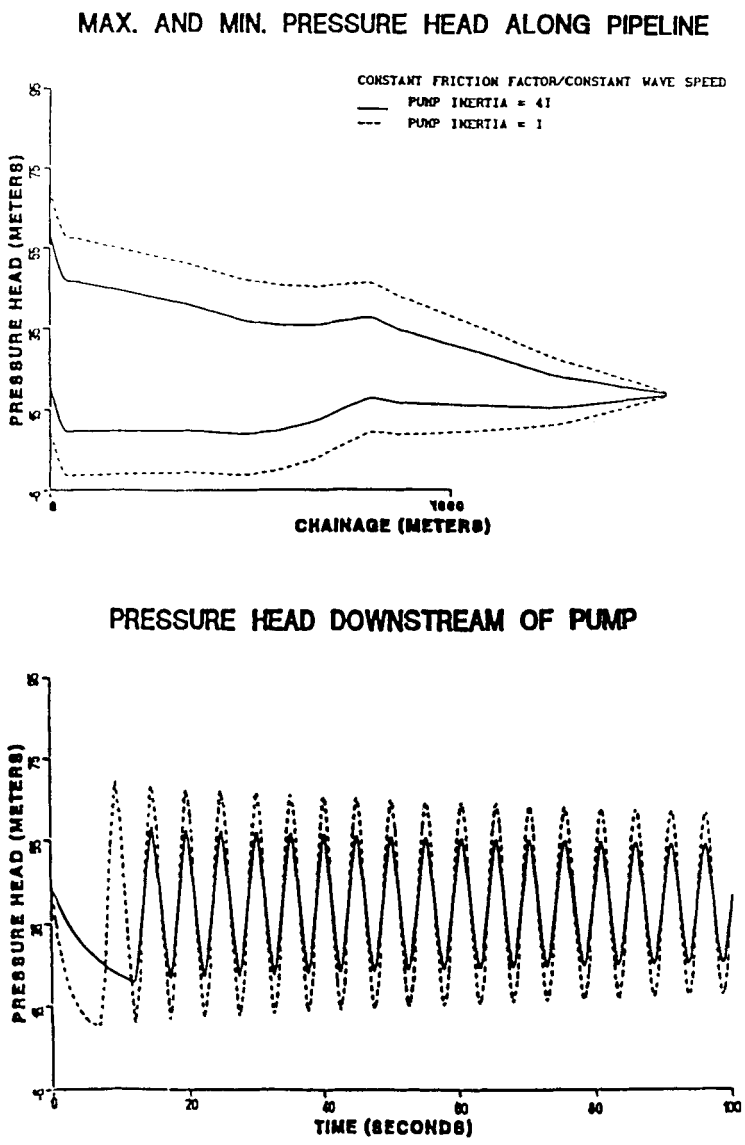

Figure 5.

studies that it is possible for a low wave speed to increase the pressure peak, even though a lower wave speed also implies a reduced change in pressure head for a given velocity change. Numerical experiments performed in this computer study also showed that the degree of amplification of the first pressure peak is dependent upon the rate of deceleration of the flow after the pump trip. An increased pump inertia produces a slower rate of deceleration of the flow after pump tripping and a smaller amplification of the first pressure peak as compared with the constant-wave-speed model. The profound effect of the variable-wave-speed model with different pump set inertias can be seen in Figures 5–7 with constant-/variable-friction models. Figure 5 shows that with constant wave speed the wave form of the transient pressure is synchronized since the period of the

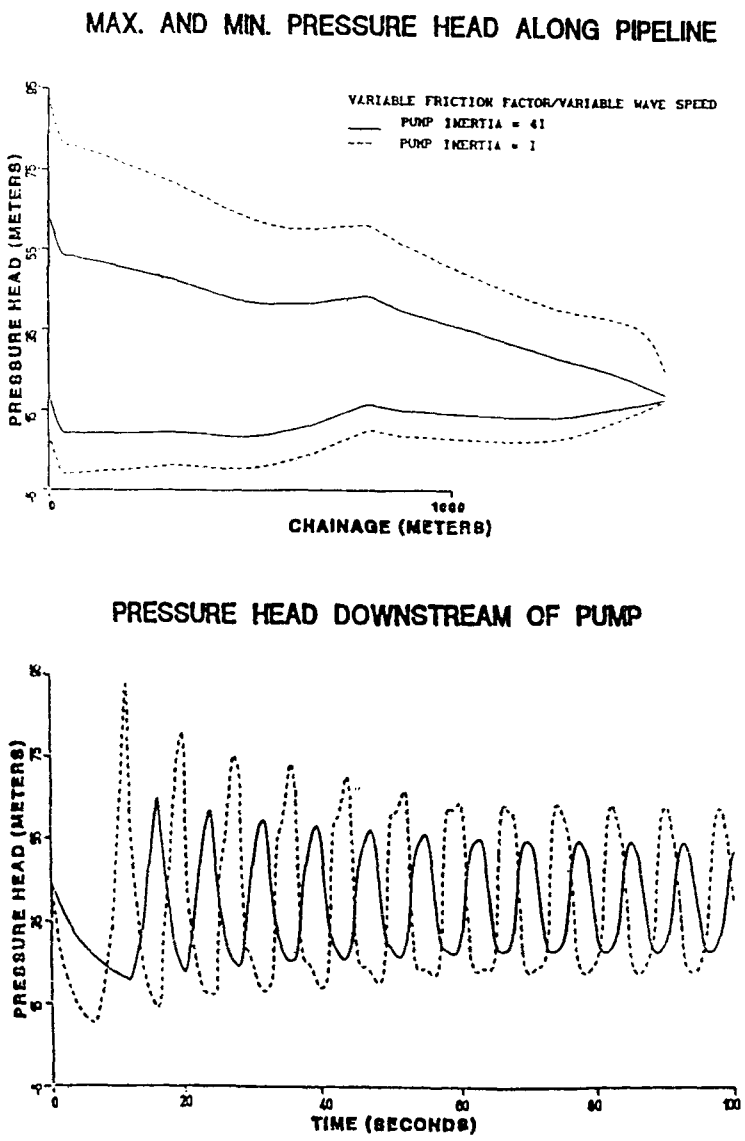

Figure 6.

pressure wave is constant. When the wave speed varies from one location to another and from one instant to another owing to the pressure variation and air content in the fluid, the period of the wave form also varies from time to time and from location to location; hence the pressure wave forms are non-synchronized in the variable-wave-speed model. Figure 8 shows that the variable-loss-factor model produces marginally higher maximum and lower minimum pressure transients when compared with the constant-loss-factor model. No significant differences in pressure surge values are seen when the transient pressures encountered are above the gas release pressure head.

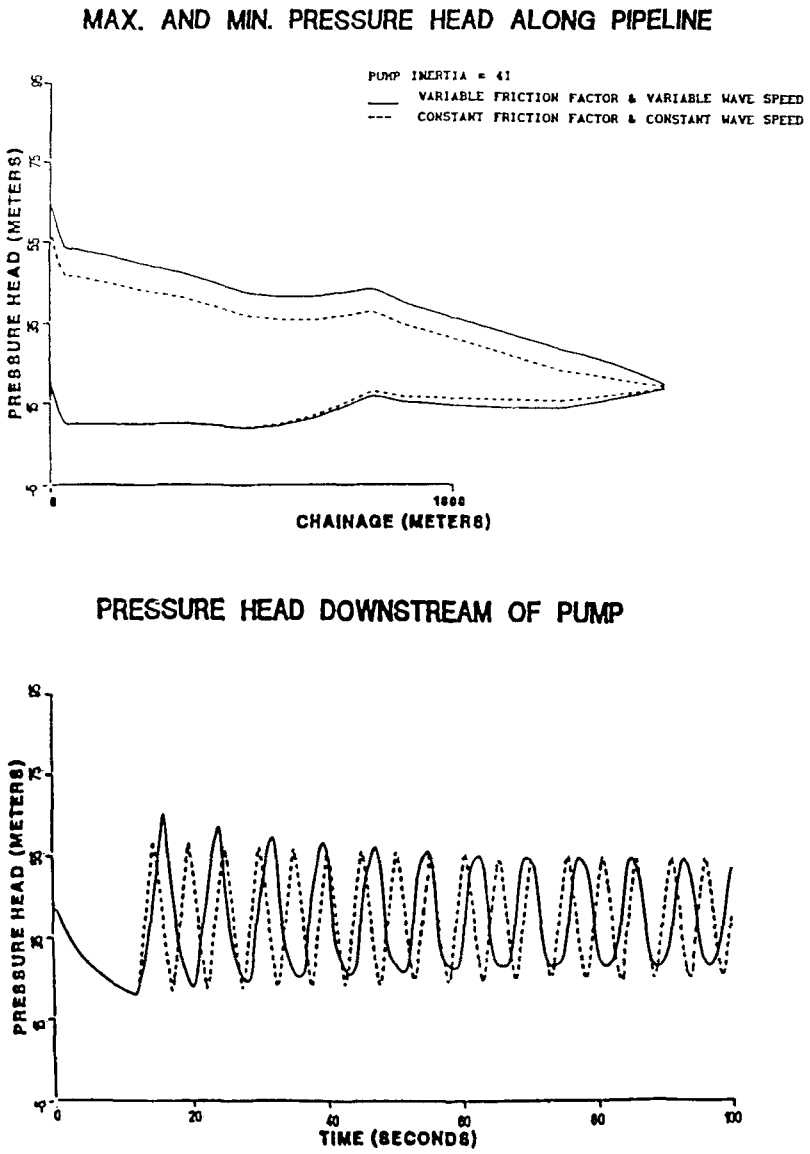

Figure 7.

From the corresponding numerical experiments it is noted that friction and any devices put into the system have a damping effect on the pressure waves owing to the hysteresis in the energy cycle. However, it is also noted that the damping produced by losses alone is small and is independent of the local surge pressure encountered. This is evident in the constant-wave-speed model where the damping of the pressure transient is slow. For the variable-wave-speed model the damping of the pressure surge is fast. This is due to the fact that the gas content ε_i at a local point will increase as the lower pressure wave is transmitted to that point during a down-surge and conversely ε_i will decrease as the higher pressure wave is transmitted to a point during the up-

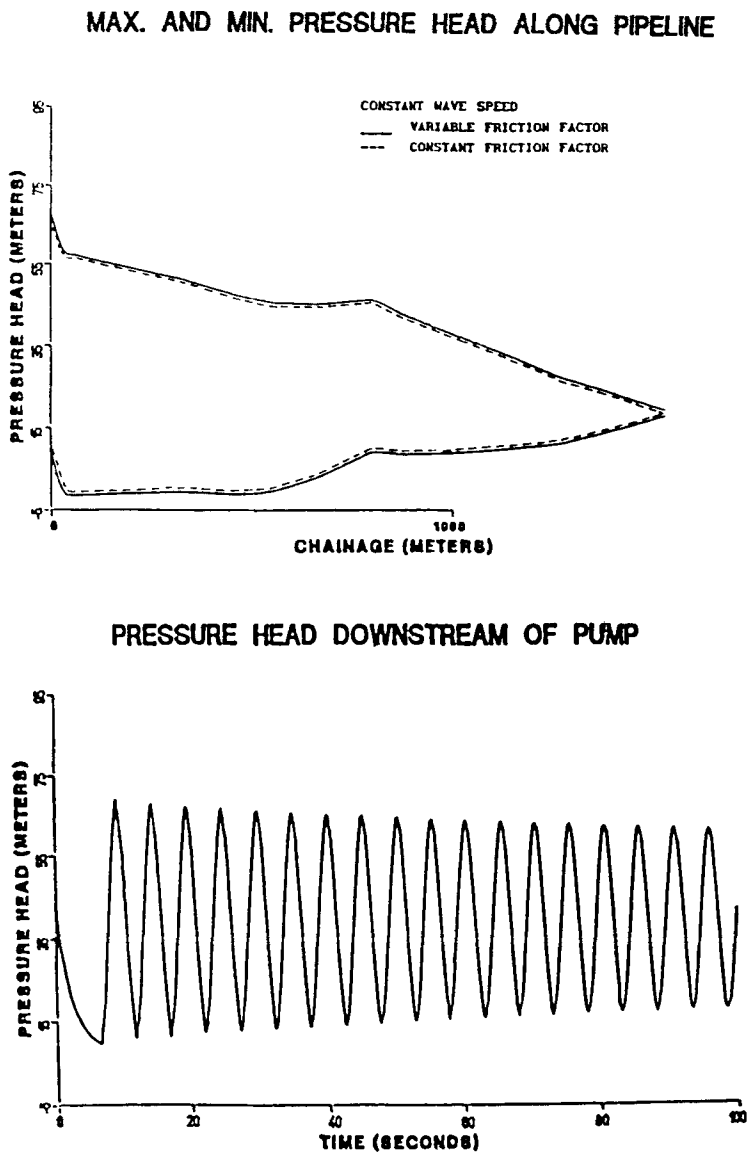

Figure 8.

surge of pressure. Hence there is an increase in the local wave speed during up-surge and a decrease in the local wave speed during down-surge. This also explains why the up-surge prediction in the variable-wave-speed model is higher than in the corresponding constant-wave-speed model and the magnitude of the down-surge prediction is smaller in the variable-wave-speed model than in the constant-wave-speed model. Generally, the numerical experiments show that the damping produced by the loss factor is much smaller than that produced by the gas content in the fluid during the pressure transient process. The precise physical cause of large surge damping in transient flow with gas content is still a subject of current research. However, possible

mechanisms have been suggested in the form of direct damping due to the increased effective bulk viscosity of the fluid as a result of the presence of air bubbles,[44] losses due to slip between bubbles and water[45] and thermodynamic losses.[8] A mechanism due to indirect damping is explained by Pearsall[22] in his reflection hypothesis, which states that when bubbly and unclear stretches of water alternate and interact, the partial wave reflections occurring at the interfaces break the periodic surge wave down. This explains the fast damping of the pressure transient in the variable-wave-speed model where air is present.

CONCLUSIONS

A numerical model and computational procedure have been developed to study the effects of air entrainment in the form of variable wave speed and variable loss factor (including friction) on the pressure transient in pumping installations. Free gas in the fluid and cavitation at the fluid vapour pressure were modelled. Numerical experiments showed that entrained, entrapped or released gases amplified the first pressure peak, increased surge damping and produced asymmetric pressure surges with respect to the static head. When air was entrained into the system, the pressure transient showed long periods of down-surge and short periods of up-surge. The up-surge was considerably amplified and the down-surge reduced in comparison to the gas-free constant-wave-speed case. These results are consistent with the experimental and field data observed by other investigators.[9,22,42,43] Numerical experiments also showed that the variable-loss-factor model produces slightly higher maximum and lower minimum pressure transients when compared with the constant-loss-factor model. They do not, however, show significant differences in pressure surge values for realistic engineering applications where the pressures encountered are usually above the fluid vapour pressure.

ACKNOWLEDGEMENTS

The author gratefully acknowledges the kind assistance of Professor H. F. Cheong, Head of Civil Engineering Department, Faculty of Engineering, National University of Singapore and the personnel from the Sewerage Department, Ministry of the Environment, Singapore for providing valuable information on pumping stations for this investigation. The support of a National University of Singapore research grant (RP0633) is also gratefully acknowledged.

APPENDIX: LIST OF SYMBOLS

a	wave speed
A_1, A_2, A_3	constants for pump H–Q curve
B_1, B_2, B_3	constants for pump T–Q curve
C_1, C_2, C_3	constants for pump η–Q curve
c	parameter describing pipe constraint condition
D	mean diameter of pipe
E	modulus of elasticity
e	local pipe wall thickness
f	friction factor
g	gravitational acceleration
H	gauge piezometric pressure head
H_g	gas release pressure head (=2·4 m water absolute)
i	node point at $x_i = (i-1)\Delta x$

I	pump set moment of inertia including flywheel
k	time level at $t_k = \sum \Delta t_k$
K	bulk modulus of elasticity
L	length of pipe
N_i^k	pump speed in rpm at node point i and time level k
N	total number of node points along the pipeline
n_p	number of pumps in a pumping station
P	pressure inside the pipe
Q	fluid flow rate
R	C^+-line intercept on x-axis at kth time level
S	C^--line intercept on x-axis at kth time level
Re	Reynolds number
T	pump torque
t	time
V	flow velocity
x	distance along pipeline
z	pipeline elevation w.r.t. pump intake level
α	pipeline inclination (positive downwards)
η	pump efficiency
τ	valve closure function
Δt_k	time step at kth time level
Δx	node point distance along pipeline
ν_s	sewage kinematic viscosity
ν_g	gas kinematic viscosity
ε	fraction of air in liquid
ε_0	fraction of free gas in liquid at atmospheric pressure
ε_g	fraction of dissolved gas in liquid
ρ	density of fluid

REFERENCES

1. K. J. Whiteman and I. S. Pearsall, 'Reflux valve and surge tests at Kingston pumping station', *Brit. Hydromech. Res. Assoc./National Engineering Laboratory Joint Report 1*, April 1959.
2. K. J. Whiteman and I. S. Pearsall, 'Reflux valve and surge tests at a station', *Fluid Handling*, **XIII**, 248–250, 282–286 (1962).
3. R. J. Brown, 'Water-column separation at two pumping plants', *J. Basic Eng., ASME*, 521–531 (1968).
4. G. A. Provoost, 'Investigation into cavitation in a prototype pipeline caused by waterhammer', *Proc. 2nd Int. Conf. on Pressures*, London, 22–24 September 1976, BHRA, Cranfield, 1976, pp. 35–43.
5. E. B. Wylie, 'Free air in liquid transient flow', *Proc. 3rd Int. Conf. on Pressure Surges*, Canterbury, March 1980, BHRA, Cranfield, 1980, pp. 12–23.
6. J. A. Fox, 'Pressure transients in pipe networks—a computer solution', *Proc. 1st Int. Conf. on Pressure Surges*, Canterbury, September 1972, BHRA, Cranfield, 1972, pp. 68–75.
7. J. A. Fox, *Hydraulic Analysis of Unsteady Flow in Pipe Network*, Macmillan, London, 1984.
8. D. J. F. Ewing, 'Allowing for free air in waterhammer analysis', *Proc. 3rd Int. Conf. on Pressure Surges*, Canterbury, March 1980, BHRA, Cranfield, 1980, pp. 80–91.
9. L. Jonsson, 'Maximum transient pressures in a conduit with check valve and air entrainment', *Proc. Int. Conf. on the Hydraulics of Pumping Stations*, Manchester, 17–19 September 1985, BHRA, Cranfield, 1985, pp. 55–76.
10. T. Kobori, S. Yokoyama and H. Miyashiro, 'Propagation velocity of pressure wave in pipe line', *Hitachi Hyoron*, **37** (10), 23–35 (1955).
11. E. Silberman, 'Some velocity attentuation in bubbly mixtures measured in standing wave tubes', *J. Acoust. Soc. Am.*, **29**, 1–12 (1957).
12. R. F. Ripken and R. M. Olsen, 'A study of the gas nuclei on cavitation scale effects in water tunnel tests', *St. Anthony Falls Hydro. Lab. Project Report 58*, University of Minnesota, Minneapolis, MN, 1958.

13. A. R. Halliwell, 'Velocity of water hammer wave in an elastic pipe', *J. Hydraul. Div., ASCE*, **89**, 40–50 (1963).
14. H. K. M. Dizkman and C. B. Vrengdenhill, 'The effects of dissolved gas on cavitation in horizontal pipelines', *J. Hydraul. Res.*, **7**, 301–313 (1969).
15. M. R. Driels, 'An investigation of pressure transients in a system containing a liquid capable of air absorption', *J. Fluid Eng., ASME*, **95**, 408–414 (1973).
16. C. Kranenburg, 'The effect of free gas on cavitation in pipelines induced by waterhammer', *Proc. 1st Int. Conf. on Pressure Surges*, Canterbury, September 1972, BHRA, Cranfield, 1972, pp. 156–163.
17. C. Kranenburg, 'Gas release during transient cavitation in pipes', *J. Hydraul. Div., ASCE*, **100**, 1383–1398 (1974).
18. C. S. Martin, 'Entrapped air in pipelines', *Proc. 2nd Int. Conf. on Pressure Surges*, London, 22–24 September 1976, BHRA, Cranfield, 1976, pp. F2-15–F2-28.
19. J. P. Tullis, V. L. Streeter and E. B. Wylie, 'Waterhammer analysis with air release', *Proc. 2nd Int. Conf. on Pressure Surges*, London, 22–24 September 1976, BHRA, Cranfield, 1976, pp. C3-35–C3-47.
20. D. C. Wiggert and M. J. Sundquist, 'The effect of gaseous cavitation in fluid transients', *J. Fluid Eng., ASME*, **101**, 79–86 (1979).
21. E. P. Evans and P. V. Saga, 'Surge analysis of a large gravity pipeline', *Proc. 4th Int. Conf. on Pressure Surges*, Bath, 21–23 September 1983, BHRA, Cranfield, 1983, pp. 447–460.
22. I. S. Pearsall, 'The velocity of water hammer waves', *Proc. Inst. Mech. Eng.*, **180**, pt. 3E, 12–20 (1965/1966).
23. T. S. Lee and H. F. Cheong, 'Fluid pressure transients with variable wavespeed and variable loss factor in sewerage pumping installations', *Proc. 3rd Japan–China Joint Conf. on Fluid Machinery*, Osaka, 23–25 April 1990, p. 2–1B. The Japan Society of Mechanical Engineers/Chinese Mechanical Engineering Society, 1990.
24. J. W. Daily, 'Resistance coefficient for accelerated and decelerated flows through smooth tubes and orifices', *ASME*, 1071–1077 (1956).
25. V. L. Streeter and C. Lai, 'Water hammer analysis including fluid friction', *J. Hydraul. Div., ASCE*, 79–112 (1962).
26. J. H. Gerrard, 'An experimental investigation on transition of turbulence in an oscillatory pipe flow', *J. Fluid Mech.*, **46**, pt. 1, 143–164 (1971).
27. T. Mizushina, T. Maruyama and H. Hirasawa, 'Structure of the turbulence in pulsating pipe flows', *J. Chem. Eng. Jpn.*, **8**, 210–216 (1975).
28. M. H. I. Baird, G. F. Round and J. N. Cardenas, 'Friction factors in pulsed turbulent flow', *Can. J. Chem. Eng.*, **49**, 220–223 (1977).
29. B. R. Ramaprian and S. W. Tu, 'An experimental study of oscillatory pipe flow at transitional Reynolds numbers', *J. Fluid Mech.*, **100**, pt. 3, 513–544 (1980).
30. Y. Kita, Y. Adachi and K. Hirose, 'Periodically oscillating turbulent flow in a pipe', *Bull. JSME*, **23**, 656–664 (1980).
31. W. Zielke, 'Frequency dependent friction in transient pipe flow', *J. Basic Eng. ASME*, 109–115 (1968).
32. F. T. Brown, 'A quasi method of characteristics with application to fluid lines with frequency dependent wall shear and heat transfer', *J. Basic Eng., ASME*, 217–227 (1969).
33. H. H. Safwat, and J. V. D. Polder, 'Friction–frequency dependence for oscillatory flows in circular pipe', *J. Hydraul. Div., ASCE*, 1933–1945 (1973).
34. Van Der Sande, 'Velocity profiles in accelerating pipe flows started from rest', *Proc. 3rd Int. Conf. on Pressure Surges*, Canterbury, March 1980, BHRA, Cranfield, 1980, pp. 235–238.
35. E. B. Shuy and C. J. Apelt, 'Friction effects in unsteady pipe flows', *Proc. 4th Int. Conf. on Pressure Surges*, Bath, 21–23 September 1983, BHRA, Cranfield, 1983, pp. 147–164.
36. L. F. Moody, 'An approximate formula for pipe friction factors', *Mech. Eng.*, **69**, 1005–1006 (1947).
37. V. L. Streeter and E. G. Wylie, *Hydraulic Transient*, FEB Press, Ann Arbor, MI, 1978.
38. E. B. Wylie and V. L. Streeter, *Fluids Transients*, McGraw-Hill, New York, 1978.
39. M. H. Chaudhry, *Applied Hydraulic Transient*, Van Nostrand Reinhold, New York, 1979.
40. E. B. Wylie, 'Advances in the use of MOC in unsteady pipeline flow', *Proc. 4th Int. Conf. on Pressure Surges*, Bath, 21–23 September 1983, BHRA, Cranfield, 1983, pp. 27–37.
41. D. S. Clarke, 'Surge suppression: a warning', *Proc. Int. Conf. on the Hydraulics of Pumping Stations*, Manchester, 17–19 September 1985, BHRA, Cranfield, 1985, pp. 39–54.
42. P. A. Dawson and J. A. Fox, 'Surge analysis and suppression techniques for a water supply scheme—a case study', *Trans. Inst. Meas. Control*, **5**, 134–142 (1983).
43. R. H. Falconer, W. Banks and J. Ellis, 'Surge pressures at Riding Mill pumping station: actual values and theoretical predictions', *Proc. 4th Int. Conf. on Pressure Surges*, Bath, 21–23 September 1983, BHRA, Cranfield, 1983, pp. 427–445.
44. G. I. Taylor, 'The coefficients of viscosity for an incompressible liquid containing air bubbles', *Proc. R. Soc. A.*, **226**, 34–39 (1954).
45. L. Van Wijngaarden, 'Some problems in the formulation of the equations for gas/liquid flows', in W. T. Koiter (ed.), *Theoretical and Applied Mechanics*, North-Holland, Amsterdam, 1976, pp. 365–372.